Maximal Cyclic Electron Flow Rate is Independent of PGRL1 in Chlamydomonas

W.J. J Nawrocki, B. Bailleul, P. Cardol, F. Rappaport, F.-A. Wollman, P. Joliot

Title:

Maximal Cyclic Electron Flow Rate is Independent of PGRL1 in Chlamydomonas

Authors:

W. J. Nawrocki[1,2,3], B. Bailleul[1], P. Cardol[2], F. Rappaport[1], F.-A. Wollman[1,*], P. Joliot[1]

[1] Institut de Biologie Physico-Chimique, UMR 7141 CNRS-UPMC, 13 rue P. et M. Curie 75005, Paris, France

[2] Laboratoire de Génétique et Physiologie des Microalgues, Institut de Botanique, Université de Liège, 4, Chemin de la Vallée, B-4000 Liège, Belgium

[3] Present address: Department of Physics and Astronomy, Vrije Universiteit Amsterdam, De Boelelaan 1081, 1081HV Amsterdam, The Netherlands;

[*] Corresponding author. E-mail: wollman@ibpc.fr

Abstract:

Cyclic electron flow (CEF) is defined as a return of the reductants from the acceptor side of Photosystem I (PSI) to the pool of its donors via the cytochrome b_6f. It is described to be complementary to the linear electron flow and essential for photosynthesis. However, despite many efforts aimed to characterize CEF, its pathway and its regulation modes remain equivocal, and its physiological significance is still not clear. Here we use novel spectroscopic to measure the rate of CEF at the onset of light in the green alga *Chlamydomonas reinhardtii*. The initial redox state of the photosynthetic chain or the oxygen concentration do not modify the initial maximal rate of CEF (60 electrons per second per PSI) but rather strongly influence its duration. Neither the maximal rate nor the duration of CEF are different in the *pgrl1* mutant compared to the wild type, disqualifying PGRL1 as the ferredoxin-plastoquinone reductase involved in the CEF mechanism.

Photosynthesis, photosystem I, cytochrome b6f, cyclic electron flow, anoxia

Highlights:

- The maximal rate of cyclic electron flow is independent of PGRL1 in vivo.

- Oxygen availability modifies the duration, but not the maximal rate of CEF.

- The rate of CEF is determined by the redox state of both PSI donor and acceptor side.

1. Introduction:

Light-dependent reactions of photosynthesis couple transfer of electrons with proton translocation across the thylakoid membrane [1]. Linear electron flow (LEF) uses 1 photon converted by each photosystem to transfer one electron from water to $NADP^+$ and to pump 3 protons to the lumen. Several other modes of electron transfer exist, which participate to the pumping of protons but have a final electron sink different from the Calvin Benson Bassham cycle. They contribute to the electrochemical proton gradient and consequently to ATP production and luminal pH [2]. Cyclic electron flow (CEF) around PSI [3] is defined as a return of reducing equivalents from the PSI acceptors pool to its donor pool through the cyt. b_6f complex. It allows the translocation of two protons for each light quantum converted by PSI but does not reduce $NADP^+$. Involvement of plastoquinone was early demonstrated since cyt. b_6f Q_O site inhibitors impeded CEF (e.g. [4]). The pathway of CEF therefore shares at least PQ, cyt. b_6f, plastocyanin (PC), PSI and Fd with that of linear electron flow. Yet, the exact pathway of the electrons from the PSI acceptors (reduced ferredoxins or NADPH) back to the thylakoid membrane is under debate, partly due to challenges of measuring CEF *in vivo* [5]. At least three pathways have been proposed to fulfil this role. The discovery that reduced Ferredoxin (Fd) is an efficient cofactor of cyclic photophosphorylation [6] led to propose that a putative Fd:PQ oxidoreductase catalyses CEF [7, 8]. PGRL1, a transmembrane thylakoid protein found in vascular plants as well as in green algae, has been suggested to fulfil this role [9]. NADH-like dehydrogenase NDH [10], a plant chloroplast homolog of mitochondrial Complex I, uses Fd or NAD(P)H to reduce plastoquinones, whereas NDA2 [11, 12] is a non-electrogenic algal NAD(P)H:PQ oxidoreductase [13]. Both enzymes are therefore potentially suited to be involved in the CEF pathway. It also was proposed by Mitchell as early as in the '70 that the part of the original Q-cycle corresponding to the PQ reducing activity at the Qi site of the b_6f could be involved in the CEF [14].

Both in the case of mutant evaluation, where one needs to assess full CEF capacity, and experiments in physiological conditions, where the actual rate and regulation of CEF is compared to the LEF, technical difficulties are yet to be overcome. CEF is notoriously challenging to gauge due to a lack of net measurable product and the intrinsic entanglement with LEF. An apparent solution to this methodological bottleneck is to block the LEF-driving PSII with inhibitors and to measure the activity of PSI either through P_{700} oxidation (e.g. [15]) or electrochromic shift measurements (e.g. [16]). However, it has been long proven wrong, as the presence of LEF determines the extent of CEF [17]. Here, we aim at obtaining the maximal rate of CEF in the green alga *Chlamydomonas reinhardtii* by focusing on the transitory period before CEF becomes electron-limited upon electron transport chain oxidation. We followed the PSI activity following the onset of light in conditions of PSII inhibition and studied the influence of a more reduced initial pool of PSI donors by using the *ptox2* mutant [18]. We then used the *pgrl1* mutant [19] to evaluate the role of the PGRL1 protein in CEF. Finally, by varying the time between consecutive illuminations or the oxygen tension, we could assess the main parameters influencing the rate and duration of this transient CEF.

2. Materials and methods:

WT (CC124), *ptox2* [18], and *pgrl1* [19] were grown at 25°C in continuous 10 μE.m^{-2}.s^{-1} light in Tris-acetate-phosphate media. Prior to each experiment, the cells from mid-log phase were spun down and resuspended in 10% (w/w) Ficoll-Minimum medium (without reduced carbon source), then dark-adapted in open Erlenmeyer flasks and shaken for at least 1 hour. Apart from the fluorescence measurements (Figs S3, S4 only), DCMU (10 μM) and hydroxylamine (1 mM) were systematically added in order to block PSII.

All the spectroscopic measurements were done using a JTS-10 spectrophotometer and orange actinic LEDs peaking at 635 nm with an intensity corresponding to 350 photons.s^{-1}.PSI^{-1} in the WT, apart from fluorescence measurements where lower light intensity was used to obtain better temporal resolution of the induction (~150 photons.s^{-1}.PSI^{-1}). Single turnover flashes used to normalize the ECS values were obtained through a dye laser (DCM, Exciton dye laser) pumped by a frequency-doubled Nd:YAG laser. P_{700} redox state was measured at 705 nm (white LEDs passing through an interference filter with 10 nm full width at half maximum) and subtraction of a corresponding measurement at 730 nm (10 nm FWHM) to remove PC-borne signals was made. ECS was monitored at 520 nm (white LEDs passing through an interference filter with 10 nm FWHM). Actinic light was cut off from the detector by long-pass Schott RG695 glass filters and BG39 Schott filters, respectively.

The oxygen measurements were performed using contactless Sensor Spots (PyroScience) stuck inside the measuring cuvette and simultaneously with the JTS-10 measurements. The sensors were calibrated before the experiments with Ficoll-Minimum medium bubbled with air for oxic condition, and with DTT added to the medium in closed cuvette for anoxic reference.

We employed the electrochromic probe of the membrane potential $\Delta\psi$ (based on the DIRK approach, Dark Interval Relaxation Kinetics, [20]) that allows determination of the photochemical rate by comparison of the electric field formation- and dissipation rates, the latter in darkness (see [20, 21] and [22] for a review). Detectable electric field across the thylakoid membrane is formed and dissipated by photosynthetic complexes in the light. Upon cessation of illumination the photochemical rate is instantly cancelled, yet on a timescale of several milliseconds the light-independent potential formation is unchanged, allowing an absolute quantification of the PSI photochemistry in the case PSII is inhibited. While charge recombination is electrogenic and contributes to the ECS signal as the electrons move from the stromal to the luminal part of the membrane, it decays rapidly in PSI [23]. By disregarding the ECS signals before 1 ms of darkness – when the vast majority of back-reactions takes place - one is able to only measure the stable rate of charge separations, i.e. 'forward' PSI photochemistry, and exclude CR, which takes place in a sub-millisecond timescale [23, 24].

The photochemical rate of PSI along the whole period of P_{700} oxidation using the ECS-based approach was measured as follows. Each timepoint corresponds to a single-turnover flash-normalised value of a difference between ECS slope in the light *minus* dark. The slopes were obtained through a linear fit of 8 1 ms-spaced detection points in the presence of actinic light, and 4 1 ms-spaced points after the light was turned off. Importantly, the first detection point

in darkness was made after 1 ms to yield the light-limited photochemical rate of PSI, before a single electron per PSI had been separated from P_{700}. Because a short, 5-ms period of darkness is necessary for the measurement for each timepoint, the measurement was split into two to avoid a significant decrease in integrated light intensity as the detection points were closely spaced. Then, either timepoints number *n*, *n+2*, *n+4*, etc. (e.g. at 10 ms, 30 ms, 80 ms...) or *n+1*, *n+3*, *n+5,* etc. (e.g. at 20 ms, 50 ms, 100 ms) were recorded. Finally, a baseline consisting of a measurement without the actinic light was subtracted from every set of data. Each of the points is a result of 5-8 technical replicates (of the same batch of algae) of the ECS measurement and averaged over 3 independent biological replicates.

The integrals of the P_{700} and ECS curves were calculated with a baseline corresponding to the redox steady-state of P_{700} in the light and to the steady-state residual PSI photochemistry, respectively. This means that unavoidably, a slight underestimation (<10%) of the number of charge separations was made in each of the cases until the steady-state was reached (Fig. 3), but neither the kinetics nor photochemical rates were affected by this treatment. For the P_{700} integrals, maximal photochemical rate obtained for each strain with the ECS measurements (initial point in the light, before a single electron per PSI had been transferred) was multiplied by the PSI yield normalised from 1 to 0 in order to obtain number of charge separations.

Hypoxia was achieved by closing the cuvette and allowing respiration to progressively consume oxygen in the sample. Typically, between 20 and 40 minutes were sufficient to induce anoxia. Fluorescence induction was measured at identical time or oxygen concentration intervals; no differences were observed between these cases, excluding any actinic effect of the 10 s light period. Apart from the inductions, the sample remained in darkness and was constantly stirred to avoid cell sedimentation. ECS measurements were systematically taken at oxygen concentrations noted in the legend of Fig. 5. Fluorescence induction curves (Fig. S3 but not S4) were normalised to the F_M acquired with a 180 ms, 10 $mE.m^{-2}.s^{-1}$ saturating pulse.

3. Results:

3.1 Transients of P_{700} oxidation reveal high P_{700} reduction rates despite PSII inhibition

In conditions of PSII inhibition (DCMU used throughout, see methods), PSI activity eventually will lead to the oxidation of all the electron carriers in the electron transfer chain, from plastoquinone to P_{700}. Given the high redox potential of P_{700}/P_{700}^{+}, P_{700}, the special chlorophyll pair of PSI, is not oxidized before the whole chain has been oxidized. In In Chlamydomonas wild type (WT) and *pgrl1* or *ptox2* mutant strains, the steady-state oxidation of P_{700} is not attained before 400 ms (Fig. 1; see also Fig. S1 for the biological variability between experiments). Given the light intensity used here (350 photons per second per PSI, see below), approximately 140 photons are captured per PSI during that period and the number of PSI charge separations can be calculated by measuring the area above the oxidation curve (see Methods). We measured approximately 40 and 31 charge separations during that period in the WT and in the *pgrl1* mutant, respectively. P_{700} stayed reduced for longer, and the charge separation value even reached 87 in the *ptox2* mutant, (Fig. 1 and Fig. 3 for statistics; see also Fig. S1). Those values are far more than the expected number of reduced compounds initially

present in the chain. This suggests that the PSI-driven oxidation of the chain is partly compensated by its light-induced reduction, which in the absence of PSII activity comes from PSI acceptors.

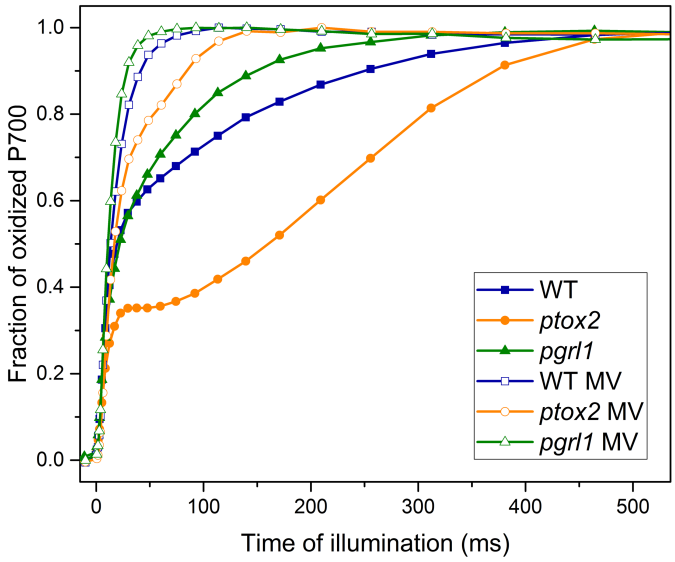

Fig. 1. Kinetics of P_{700} oxidation upon dark-to-light transition depends on PSI electron donors and acceptors. The different curves correspond to the WT (blue), the *pgrl1* mutant (green) and the *ptox2* mutant (orange), in the presence (closed symbols) or absence (open symbols) of 6 mM methyl viologen. DCMU and hydroxylamine were added to all of the samples. Light intensity corresponds to ~350 photons.s^{-1}.PSI^{-1}. Averages of 3 independent measurements are shown. Related statistics are shown in Fig. 3.

To test this, we measured the P_{700} oxidation kinetics in conditions preventing any reducing pressure on the photosynthetic chain from PSI acceptors. We used an artificial electron acceptor for PSI, methyl viologen (MV; paraquat). The E_M of about -690 mV of MV allows its di-cation form to be reduced by F_B, the terminal iron-sulphur cluster in PSI, but not to oxidize the PQ pool. In these conditions, no light-induced reduction of the chain can occur and each PSI charge separation leads to the net oxidation of one electron carrier in the photosynthetic chain. As shown in Fig. 1 (quantification and statistics are presented in the Fig. 3), the oxidation of P_{700} was much faster in the presence of MV and the area above the curve represents the number of electrons initially present in the chain. We measured 11, 9 and 20 electrons on the PSI donor side in the WT, the *pgrl1* mutant and the *ptox2* mutant, respectively. The large difference in the number of PSI charge separations required to fully oxidize the chain, with or without MV, confirms that a reduction pathway(s) take place concomitantly to the PSI-driven oxidation of the chain (that we will call LEF in the following). Such a light-dependent reduction pathway must involve PSI acceptors, since PSII is inactive here, which leaves us with two candidates: a direct P_{700}^+ reduction through charge recombination and CEF.

3.2 ECS-based measurements of photochemical rate allow discrimination between CEF and PSI charge recombination

In those two processes, P_{700} will be alternately oxidized and reduced (by PSI primary acceptor in the case of CR, by plastocyanin in the case of CEF). But the consequences will be different from an electric standpoint: only a stable charge separation (*i.e.* one that does not recombine within the millisecond time range) will contribute to an increase of the transmembrane electric field, as a positive charge will remain in the lumen.

Therefore, to discriminate between CEF and charge recombination on a kinetic basis, we used a method based on the electrochromic shift (ECS) of the photosynthetic pigments, which is a probe of the membrane potential [20-22]. The method consists in repeated measurements of PSI photochemical rate (see methods for technical details) and allows to count only stable charge separation events, i.e. to disregard charge recombination which occur faster [23]. The results of these measurements are presented in Fig. 2. The first plotted point (1 ms after the onset of light) corresponds to the light-limited PSI rate (i.e. when only the light absorption limits the photochemistry of PSI). The initial rate of PSI in the *ptox2* mutant is higher, as shown before [25], due to its lock in state II in darkness [18], where LHCIIs increase PSI cross-section [26]. Subsequently, the rate decreases to a steady-state level in all three strains. In the first 80 ms of illumination – called the first phase hereafter - we observed only minor differences in rates between the WT and *pgrl1* (or *pgr5*, Fig. S2) and a normalisation of the *ptox2* mutant curve to the initial PSI rate in the WT alleviates the differences in rates during this phase (see Fig. S3). High PSI rates are maintained for a longer period in *ptox2* during the second phase of illumination (*i.e.* after 80 ms). As discussed later, we interpret this phase as a prolongation of the concomitant presence of CEF and LEF due to an increased number of PSI electron donors initially present in the thylakoid membrane.

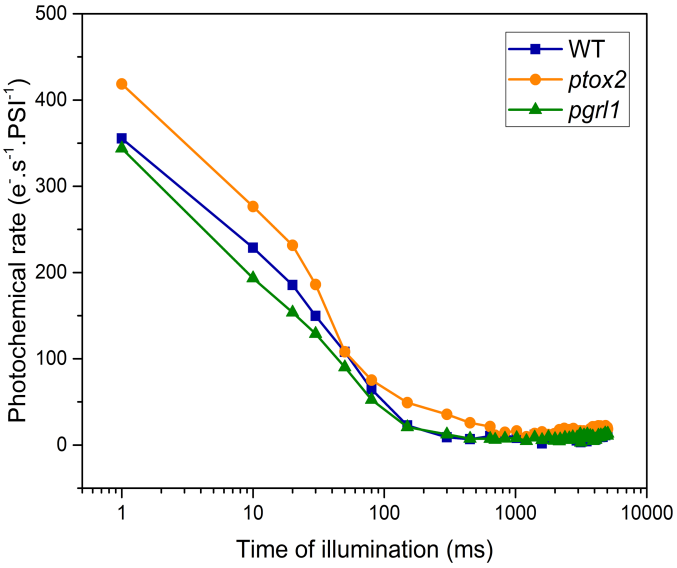

Fig. 2. Number of PSI electron donors directly influences the decay of the photochemical rate of PSI during dark-to-light transition. WT (blue), the *pgrl1* mutant (green) and the *ptox2* mutant (orange) were assessed in the presence of DCMU and hydroxylamine. PSI photochemical rates are calculated through the change of slope of the ECS signal at the offset of light

normalized by the saturating flash-induced ECS (see Methods). Each timepoint is an average of 3 biological replicates.

3.3 Comparing ECS and P_{700} measurements allows the estimation of the total LEF, CEF and charge recombination events.

An integration of the PSI photochemical rate over time until the steady-state is achieved yields the number of stable charge separations performed by PSI. This sums the electrons actually transferred per PSI by both LEF and CEF (Fig. 3). Expectedly for the three strains, the values of this integral (LEF+CEF, Fig. 2) fall in between the number of total PSI charge separations (LEF+CEF+CR; Fig. 1, without MV) and the number of initial donors in the pool (LEF only; Fig. 1, with MV). In our conditions, roughly half of the total PSI charge separations correspond to charge recombinations, regardless of the strain. While this is a surprising observation, we note that the CR/LEF ratio is here exacerbated compared to steady-state photosynthesis, as the measurements are performed in dark-adapted cells (e.g. CBB cycle inactive) subjected to high light.

We did not observe significant difference between the integrals of the WT and the *pgrl1* mutant. In contrast, more electrons were initially present in the pool of PSI donors in the *ptox2* mutant, which, in turn, increased both the activity of CEF and the quantity of charge recombinations. While the logarithmic scale used in Fig. 2 and Fig S3 is not well suited for the discrimination of differences in the areas, it is important to note here that the difference between the *ptox2* mutant and the WT originates mostly from the second phase and not from the first phase (the difference in the first phase corresponds to only 1 or 2 electrons transferred).

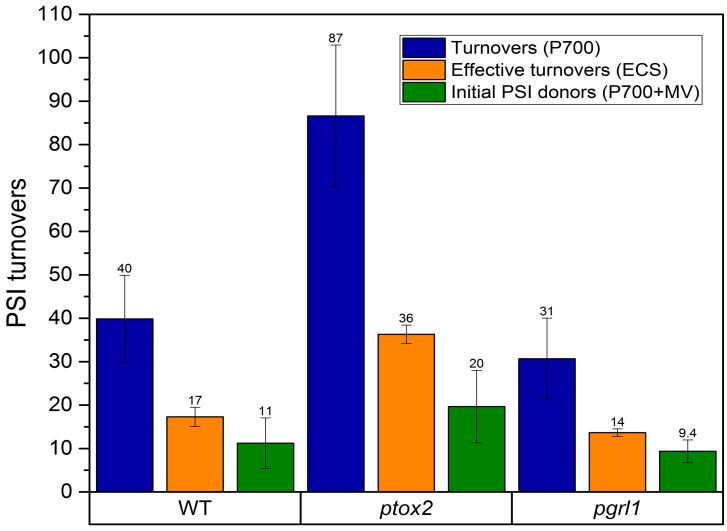

Fig. 3. Quantification of the PSI charge separations upon dark-to-light transition in oxic conditions until a redox steady-state is attained. Total charge separations (blue, corresponding to LEF+CEF+CR), stable charge separations (orange, corresponding to LEF+CEF) and initial electron number (green, only LEF) are shown. Means ± SDs of 3 (P_{700}, P_{700}+MV) or 8 (ECS) independent experiments are shown.

3.4 CEF activity depends on the initial number of PSI donors and acceptors

The results above suggest that the extent of CEF and CR depend on the initial amount of reducing equivalents in the electron transfer chain (i.e. more CEF and more CR in the *ptox2* mutant). To further test this, instead of relying on mutants, we modified the initial number of electrons in the electron transfer chain (ETC) with prior illumination. Just after a pre-illumination in the presence of DCMU, the ETC will be fully oxidized, and from then it will get more and more reduced with time in the dark because of the activity of NDA2. The duration after the pre-illumination therefore modulates the initial number of PSI donors, which we can measure through the area below the P_{700} oxidation curves in the presence of MV (like in Fig. 1). This number increases with time in all strains (Fig. 4C) and the process is finished when cells are given around 10 seconds of relaxation in darkness after the first illumination. Once a steady state is achieved, the number of reducing equivalents in the ETC is virtually identical in the WT and *pgrl1* mutant, but higher in the *ptox2* mutant because of the absence of the plastoquinol oxidizing activity of PTOX2.

Using the same protocol as for Fig. 1 and Fig. 2, we could show that, during the first ten seconds, the number of charge recombination and the activity of the CEF increase concomitantly with the initial number of reducing equivalents in the ETC. More precisely, the number of charge separations leading to charge recombinations can be obtained from the difference between the total charge separations (Fig. 4A) and the stable charge separations (Fig. 4B). The ones corresponding to CEF can be calculated from the difference between stable charge separations (Fig. 4B) and the initial number of reducing equivalents (Fig. 4C). At the end of the phase of reduction of the ETC (10 s), this leads to approximately 125, 80 and 55 charge recombination events and approximately 35, 20 and 15 PSI charge separations involved in CEF in the *ptox*2, wt and *pgrl1* strains, respectively. These results indicate that the amounts of CR and CEF strongly depend on the initial number of PSI donors in the ETC. However, in a second phase (10 – 60 s between illuminations), the total (Fig. 4A) and stable (Fig 4B) PSI charge separations start to decrease with the delay between illuminations in the WT and the *pgrl1*. We interpret the decrease of CEF and CR after 10 s as a chlororespiration-mediated oxidation of PSI acceptors, which decreases the probability of charge recombinations and CEF. In agreement with this view, the decrease is attenuated in the *ptox2* mutant where such a PTOX2-dependent oxidation of PSI acceptors does not occur. Therefore, in a given physiological condition, the duration and extent of both CEF and CR during the dark-to-light transition are strongly dependent on the initial number of both PSI donors and acceptors. There are small but significant differences between the WT and the *pgrl1* mutant in terms of CEF (Fig 4B) when light phases are given 10-60 s apart. This could reflect the regulatory role of PGRL1 in CEF, but a decrease in the CEF-related re-oxidation of the PSI acceptors should be accompanied by an increase in charge recombination rate. We observe the opposite effect (Fig 4A). Given the strong and complex dependence of CEF and CR on the initial pool of PSI donors and acceptors, we favor an alternative hypothesis, that the difference between WT and *pgrl1* mutant arises from small differences in the relaxation of the redox state of the chain. We demonstrated that a more reduced pool of PSI donors and/or acceptors increases both CEF and CR in the *ptox2* mutant. In the same way, a more oxidized pool of PSI donors and/or acceptors at a given time would indeed tend to decrease both CEF and CR in the *pgrl1* mutant compared to the WT.

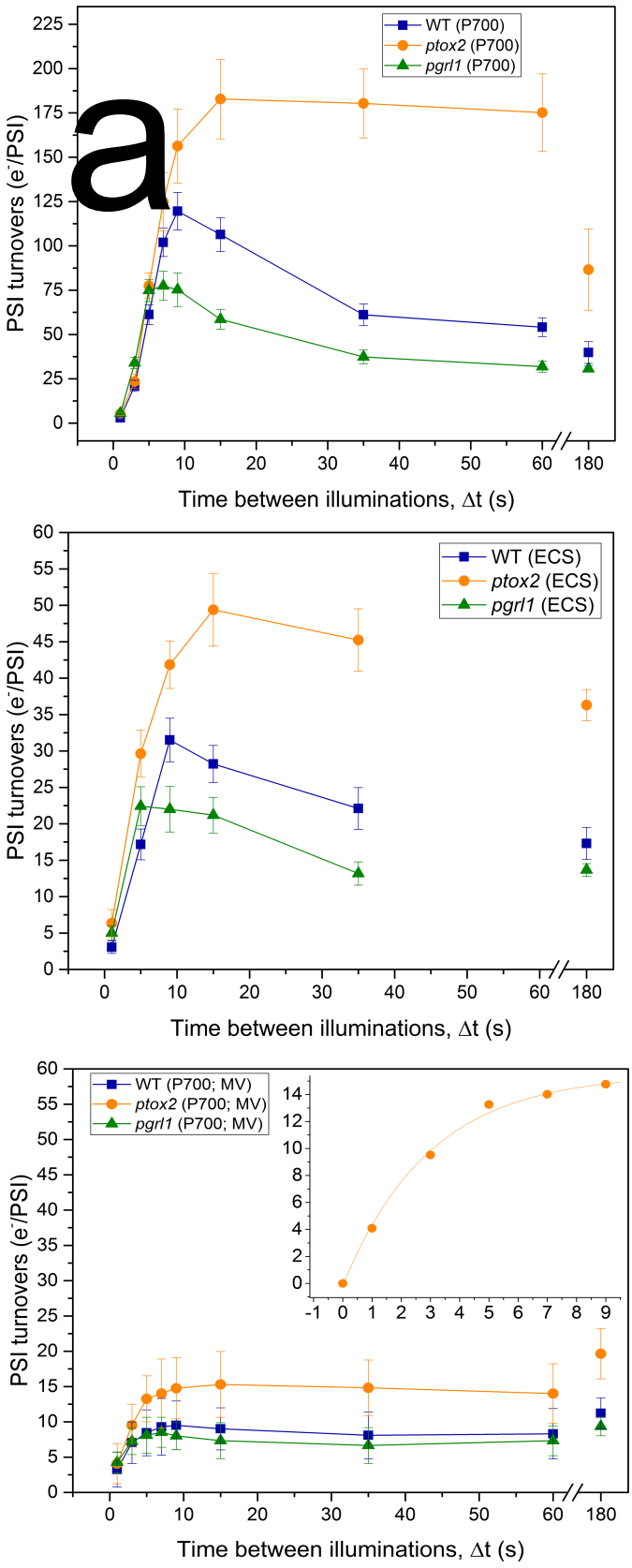

Fig. 4. Preillumination allows studying the kinetics of electron transfer chain reduction in darkness. Dependence of the PSI activity upon the delay between consecutive illuminations in the WT (blue), the *pgrl1* mutant (green) and the *ptox2* mutant (orange). A-B: Evolution of the total (A) and stable (B) PSI charge separations before steady-state P_{700} oxidation, depending

on the delay between consecutive illuminations. C: Initial number of reducing equivalents in the ETC as a function of the delay between consecutive illuminations. Here, the reduction of the ETC reflects the sole activity of NDA2 was fitted with a mono-exponential function (inset). The maximal rate of NDA2 was around 4 $e^-.s^{-1}.PSI^{-1}$, slightly higher than the one obtained beforehand with a fluorescence-based approach in a b_6f -lacking mutant (2 - 2.4 $e^-.s^{-1}.PSI^{-1}$; [18]).All experiments were performed in the presence of DCMU and hydroxylamine, an each timepoint is an average of 3 biological replicates ± S.D.

The data presented above indicate that some CEF takes place during the dark-to-light transition. This is especially prominent when two illuminations are given 10 s apart, allowing during the dark period between them a full reduction of the PSI donors but only a partial reoxidation of the PSI acceptors. In these conditions, in the WT and the *pgrl1* mutant (and regardless of the delay between illuminations for the *ptox2* mutant), the difference between the number of stable charge separations (CEF + LEF) and the number of charge separations in the presence of MV represents a statistically significant number of PSI charge separation events leading to CEF. The differences between these timepoints suggest that in *pgrl1* there is less CEF *and* CR compared to WT upon PSI oxidation. Importantly, as discussed above, this suggests some redox differences on the acceptor side of the PSI rather than simply less CEF.

However, those values are integrated over the duration of the transient and do not directly express the rates of each process. To evaluate the rate of charge recombination at any time during the transient, one can subtract the photochemical rate to the PSI charge separation rate based on P_{700} oxidation curve (e.g. Fig. S3 for dark-adapted samples). It is visible that during the first phase of P_{700} oxidation, completed in 25 ms, the rates of total (P_{700}-based) and stable (ECS-based) PSI charge separations are identical in the WT and *ptox2*, suggesting that electron transfer from PSI donors to PSI acceptors (LEF) occurs in this period. Next, the divergence of the two curves indicates that CR becomes a prominent process. For example, 100 ms after the onset of light, the charge recombination rates are ~150 and ~250 $e^-.s^{-1}.PSI^{-1}$ in the WT and the *ptox2* mutant, respectively (Fig. S3). In contrast, the calculation of CEF rates is more challenging because the number of stable PSI charge separations during the transitory phase is still an entanglement of CEF and LEF (i.e. the oxidation of the initial PSI donor pool).

3.5 Varying the oxygen tension allows prolongation of the rapid transitory CEF

It has been previously shown that P_{700} oxidation is lengthy in low oxygen concentration conditions, with the extreme case being anoxia where P_{700} remains reduced for several seconds [27]. It also has long been known that CEF is enhanced when the oxygen concentration decreases (e.g. [25, 27, 28]). Under low oxygen tension, the lower activity of mitochondrial and chloroplast oxidases generates a high concentration of reduced compounds in the cell, and especially a higher reduction of both the plastoquinone pool and of the PSI acceptors. Therefore, we reasoned that the changes in the initial redox state of the chain in hypoxic conditions would lead to a higher and longer transitory CEF, allowing us to discriminate it better from LEF. Here we apply the new approach presented above in a range of oxygen concentrations in a bid to obtain the maximal rate of CEF (CEF_{Max}) (Fig. 5).

As the oxygen concentration decreases, the duration of the transitory phase increases in all strains. A steady-state is attained in 400 ms in oxic conditions, in agreement with previous observations (see Figs 1 and 2). In contrast, at 10 µM O_2, it took 1.5 seconds for the WT and the *pgrl1* mutant and even 3 seconds in the *ptox2* mutant to reach this steady-state. When the oxygen tension was below 42 µM, the photochemical rate reached a transitory plateau corresponding to ~60 electrons transferred per second per PSI. Because the photochemical rate at the plateau was the same regardless of the oxygen tension and regardless of the strain, we conclude that this value corresponds to CEF_{Max}, the maximal rate of CEF in dark-adapted *Chlamydomonas reinhardtii*. While the photochemical rate at the plateau was independent of the strain or oxygen tension, the duration of the plateau varied depending on the strain and degree of hypoxia. Regardless of the oxygen tension, the plateau at 60 $e^-.s^{-1}.PSI^{-1}$ lasted longer in the *ptox2* mutant than in the two other strains, and its duration was also longer as the oxygen decreased in all strains. This again indicates that the transitory CEF strongly depends on the initial redox state of the electron transfer chain. Importantly, the overall kinetics and absolute values are virtually identical in the *pgrl1* mutant to those in hypoxic WT, similarly to the situation in oxia (Figs 2, 4 and 5), indicating that the capacity for CEF is not affected in the absence of PGRL1. This means that PGRL1 is not directly involved in the CEF itself and that the higher rates of CEF measured in this strain in anoxia in the past [29] are due to an indirect role of this protein instead.

The activities of many oxidases are expected to decrease under hypoxia and could explain changes in CEF rate and duration. Given the high affinity of mitochondrial oxidases for oxygen (the kinetic order of reaction for oxygen in respiration is 0), their activity would not change in the range of oxygen concentrations explored here. In contrast, several chloroplast oxidases could be involved in the extension of the PSI activity under hypoxia. Because those oxidases participate in the oxidation of photosynthetic electron carriers, a decrease of their activity would lead to an over-reduction of PSI donors and/or acceptors. This, as we have seen above, would tend to increase the transitory CEF. In addition, such oxidases (flavo di-iron proteins, Mehler reaction) might also be involved in the oxidation of the PSI acceptors during the transient, which would also modify the time it takes for the chain to be fully oxidized and thereof the extent of CEF. To understand better the interplay between oxygen, oxidases and the extent of CEF, we have measured fluorescence induction kinetics under different oxygen tensions (Figs S4, S5). In oxic conditions, fluorescence first increased from the F_0 level to a transitory maximal level close to F_M. This phase (below 500 ms, Fig. S4A) was very similar in the different measurements and only a minor increase of the F_0 was observed, as oxygen concentration decreased (apart from anoxia – 0 µM O_2 – where the F_0 rise was significant). Therefore, it seems unlikely that the increase of CEF under hypoxia stems from chlororespiration-dependent changes in the initial number of electrons in the ETC, as confirmed by the observed differences stemming from the absence of PTOX2 in oxia (Fig. 3) and the lack of correlation between F_V/F_M parameter and the increase of CEF duration (Fig. S5). After 500 ms, a decrease of fluorescence until a steady-state value is reached, takes place in oxic conditions, which reflects the activation of a photosynthetic electron sink. Its suppression in hypoxic conditions (Fig. S4B; Φ_{PSII} in Fig. S5) suggests that this electron sink corresponds to the activity of a chloroplast oxidase. These results together with the ECS-based measurements presented in Fig. 5 suggest

that the progressive increase in CEF duration in hypoxia is due to the decrease of activity of a chloroplast oxidase, involved in the reoxidation of PSI acceptors during the transient, and provide a parsimonious interpretation to the previously observed "induction" of CEF in anoxia.

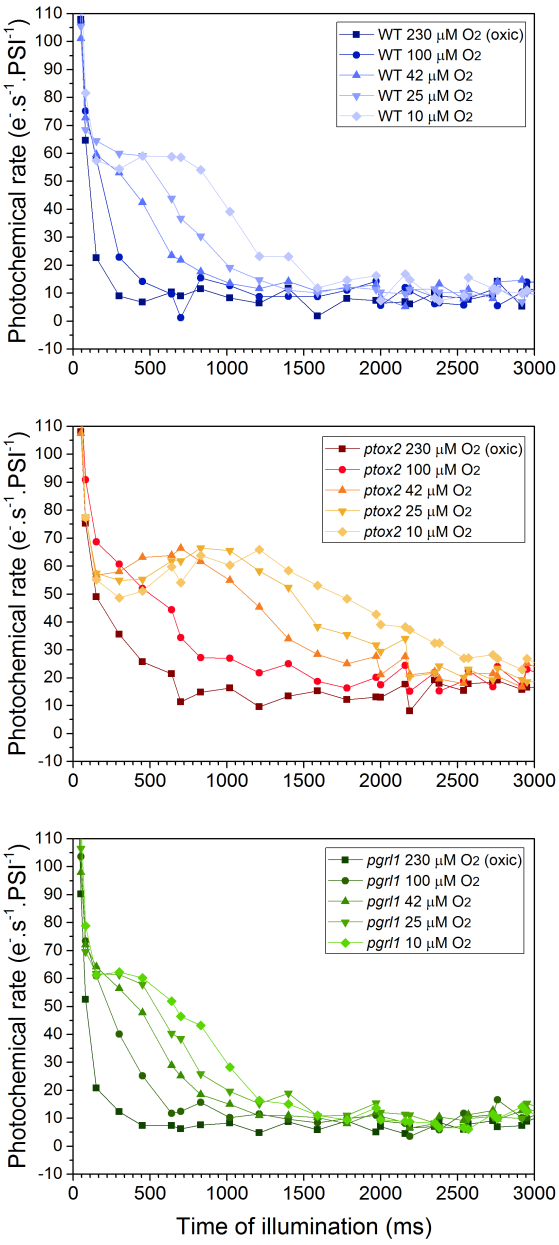

Fig. 5. Photochemical rate of PSI during a dark-to-light transition in the presence of DCMU, under different oxygen concentrations. The first point is not shown, see text for details and full extent of the measurements in the Fig. S6. Each timepoint is an average of 3 biological replicates.

4. Discussion:

The complex relation between LEF and CEF renders studies of mechanism and regulation of CEF highly complicated. On one hand, CEF and LEF directly compete for several intermediate electron carriers. From this point of view, the activity of LEF limits the steady-state value of CEF. On the other hand, in the absence of LEF, CEF rapidly slows down because of the

unavoidable leaks of electrons from CEF through the many pathways fuelled by reduced photosynthetic electron carriers. This is especially apparent in the results presented in Fig. 5: after the period of constant and maximal rate of CEF (60 $e^-.s^{-1}.PSI^{-1}$), the latter slowly decreased to a far smaller steady-state value. In vascular plants, this drawback is overcome through the use of far-red light which is absorbed with a higher efficiency by PSI (by low-energy chlorophylls in LHCa) than by PSII. In this case, the small electron leak to downstream reactions is compensated by PSII activity without compromising PSI activity. In these conditions, high CEF rates (up to 130 $e^-.s^{-1}.PSI^{-1}$) have been observed [24]. In *Chlamydomonas*, the difference between the absorption spectra of the two photosystems is too small in the far-red region to apply the same method [30, 31]. We approached this difficulty by focusing on a transient situation where LEF, blocked by DCMU, cannot compete with CEF. At the same time, we modulated the initial pool of electron donors in the ETC so that CEF can reach its maximal value before leaks tend to fully oxidize the ETC, limiting CEF. In a first approach we varied the delay between two consecutive illuminations. The second one consisted in affecting the activity of chloroplast oxidases, through the use of a *ptox2* strain, which lacks the major PQ oxidase, and through the modulation of the oxygen tension in the medium. Then, the measurements of P_{700} oxidation transients and ECS-based PSI photochemical rates allowed us to determine the total and stable PSI charge separations until the steady state was reached. By adding an artificial PSI electron acceptor, we could also quantify the number of electrons initially present in the PSI donors (PQ, plastocyanin, cyt. *f*, Rieske protein). Together, these measurements provided the amount of PSI charge separations leading to net oxidation of PSI donors, cyclic electron flow and charge recombination.

The measurements indicate that the amount of CEF and CR increased with the initial number of electrons on the donor side of PSI. This was supported by the increase of CR and CEF in the *ptox2* strain compared to the WT and *pgrl1* strain. Starting from a fully oxidized chain after a first illumination, CR and CEF also increased when the delay given to chlororespiration to reduce the ETC was increased (from 0 to 10 s). But our results indicate that the amount of CEF and CR depend on the redox state of the acceptor side of PSI. Indeed, when the delay between two consecutive illuminations was prolonged after the reduction of the PSI donors reached a steady-state, then the amount of CEF and CR decreased again, which we interpret as an oxidation of the PSI acceptors through the combined activities of NDA2 and PTOX. We also observed that lowering the oxygen tension in our sample decreased the rate of PSI acceptors reoxidation and increased CEF rates and duration. Taken together, these observations indicate that CEF is favoured by both PSI donors and PSI acceptors reduction: CEF will occur as soon as the PSI acceptor side is reduced (at the end of the first phase, i.e. after ~80 ms) and will slow-down when the ETC gets too oxidized to provide P_{700}^+ with electrons at a sufficient rate. Therefore, to fulfil the requirements of an experimental setup for CEF_{Max} measurements, one needs to ensure a high level of reduction of the ETC, a slow reoxidation rate of the PSI acceptors in the light, together with a proper methodology allowing the measurement of stable PSI charge separations (disregarding the charge recombination events).

Under lowered oxygen tension and in the presence of DCMU, we obtained a time window during which CEF proceeds at its maximal rate, in the order of 60 $e^-.s^{-1}.PSI^{-1}$. This value interestingly

corresponds to the highest value reported in the literature for *Chlamydomonas reinhardtii* [29]. We were able to increase the duration of CEF_{Max} in hypoxic conditions for up to 3 seconds. Importantly, this prolongation increases steadily with the oxygen depletion mediated by mitochondrial respiration, *i.e.* does not suddenly occur after some threshold oxygen concentration. We interpret this as a suppression of an O_2-dependent pathway of reoxidation of PSI acceptors. We exclude the involvement of the Mehler reaction, a direct oxygen reduction by the PSI F_A/F_B ISCs, because it is not sensitive to oxygen in our range of concentrations. Nonetheless, the flavo di-iron proteins (Flvs), recently discovered in Chlamydomonas [32, 33] are good candidates for this role. Indeed, in angiosperms - where Flvs are absent - the PSI oxidation lag in the presence of DCMU is lengthy [24], similarly to moss strains lacking Flvs [34]. If so, the oxygen titration presented above is a demonstration that the affinity of Flv for oxygen has an apparent K_M of ~15 µM in vivo, in line with previous estimates attributing this value to the Mehler reaction [35]. However, we cannot rule out that a deactivation of the Calvin-Benson-Bassham cycle itself, as oxygen decreases, explains in part the decrease in the rate of reoxidation of the PSI acceptors. According to our data, CEF is not 'activated' to compensate for the lack of Flvs [34], but rather the leak of electrons from the electron transfer chain to oxygen is suppressed until the Calvin Benson Bassham cycle activates and provides such role.

One of the major outcomes of this work is that PGRL1 is not involved mechanistically in CEF. This conclusion is supported by the maintenance of the maximal rate of CEF in the *pgrl1* mutant at the same level as in the WT. Together with the previously demonstrated indirect role of PGR5 in CEF in vascular plants [36], this constitutes the final piece of puzzle of the involvement of the PGRL1/PGR5 pathway in CEF. In our view, these two proteins influence the extent of CEF in physiological conditions [16, 29, 36-40], yet they do not mediate this pathway directly, i.e. they are not involved as cofactors of the electron transfer to the PQ. This is supported by the observation that the duration of CEF is slightly shorter in the *pgrl1* mutant in anoxia (Fig. 5). Thus, PGRL1 is not the putative ferredoxin-plastoquinone oxidoreductase. It is now crucial to revisit the actual pathway of the CEF in plants and green algae. As described in detail in the accompanying Perspective Article [41], the main alternative pathway to the "PGRL1/PGR5-dependent" one involves NDH/NDA2. The kinetic information about the maximal rates these enzymes can achieve completely excludes them from being directly involved in rapid CEF. With rates of around 2-4 and 0.2 $e^-.s^{-1}.PSI^{-1}$, respectively, their contribution is one to two orders of magnitude too small to account for the observed CEF_{Max}. We therefore favour the original idea of Mitchell, mostly overlooked by the community, that a direct PQ reduction mediated by the cyt. b_6f is the main pathway from PSI acceptors to the thylakoid membrane in CEF [24]. Such pathway would then be regulated, in oxidizing conditions, by the PGRL1/PGR5 couple, but the way this is achieved remains to be demonstrated.

Another major conclusion of this study is that the extent of CEF can be modulated from very low values (in steady-state oxic conditions) to the maximal values reported in the literature [29] by modulating only the redox state of the PSI donors and acceptors, i.e. without the requirement of supramolecular reorganization of the membrane or higher degree of redox regulation. However, the latter can still occur *in vivo*, in order to modulate the relative activities of the LEF and CEF. If the LEF and CEF chains are spatially separated, LEF/CEF ratio can be modulated by

changing the extent of this separation (see discussion in the perspective article). Nonetheless, in our view, the increased rates of CEF in anoxia observed previously [25, 27-29, 42, 43] did not necessarily occur because of differences in structuration or redox regulation of some CEF enzymes, as usually proposed. The models for a passive regulation of the CEF through the redox states of the PQ pool and/or PSI acceptors only, are less abundant [2, 44]. However, it seems important to us to keep considering such a parsimonious model when interpreting CEF data.

Acknowledgements, statements:

W.J.N was supported by French Ministry of Education. P.C is a Senior Research Associate from Belgian F.R.S.-FNRS. The authors acknowledge funding from the ERC (consolidator grant BEAL 682580), French state (Labex DYNAMO ANR-11-LABX-0011-01), CNRS and UPMC.

The authors declare no conflicts of interest.

Author contributions:

W.J.N. performed all the experiments. All the authors analysed the data and wrote the manuscript.

5. References:

[1] S. Eberhard, G. Finazzi, F.A. Wollman, The dynamics of photosynthesis, Annual review of genetics 42 (2008) 463-515.
[2] J.F. Allen, Cyclic, pseudocyclic and noncyclic photophosphorylation: new links in the chain, Trends in plant science 8(1) (2003) 15-9.
[3] D.I. Arnon, M.B. Allen, F.R. Whatley, Photosynthesis by isolated chloroplasts, Nature 174(4426) (1954) 394-6.
[4] R.E. Cleland, D.S. Bendall, Photosystem I cyclic electron transport: Measurement of ferredoxin-plastoquinone reductase activity, Photosynthesis research 34(3) (1992) 409-18.
[5] D.Y. Fan, D. Fitzpatrick, R. Oguchi, W. Ma, J. Kou, W.S. Chow, Obstacles in the quantification of the cyclic electron flux around Photosystem I in leaves of C3 plants, Photosynthesis research 129(3) (2016) 239-51.
[6] K. Tagawa, H.Y. Tsujimoto, D.I. Arnon, Role of chloroplast ferredoxin in the energy conversion process of photosynthesis, Proceedings of the National Academy of Sciences of the United States of America 49 (1963) 567-72.
[7] R.E. Cleland, D.S. Bendall, Photosystem I cyclic electron transport: Measurement of ferredoxin-plastoquinone reductase activity, Photosynthesis research 34(3) (1992) 409-418.
[8] D.A. Moss, D.S. Bendall, Cyclic electron transport in chloroplasts. The Q-cycle and the site of action of antimycin, Biochimica et Biophysica Acta (BBA) - Bioenergetics 767(3) (1984) 389-395.
[9] A.P. Hertle, T. Blunder, T. Wunder, P. Pesaresi, M. Pribil, U. Armbruster, D. Leister, PGRL1 is the elusive ferredoxin-plastoquinone reductase in photosynthetic cyclic electron flow, Molecular cell 49(3) (2013) 511-23.
[10] H. Yamamoto, L. Peng, Y. Fukao, T. Shikanai, An Src homology 3 domain-like fold protein forms a ferredoxin binding site for the chloroplast NADH dehydrogenase-like complex in Arabidopsis, The Plant cell 23(4) (2011) 1480-93.
[11] C. Desplats, F. Mus, S. Cuine, E. Billon, L. Cournac, G. Peltier, Characterization of Nda2, a plastoquinone-reducing type II NAD(P)H dehydrogenase in chlamydomonas chloroplasts, The Journal of biological chemistry 284(7) (2009) 4148-57.
[12] F. Jans, E. Mignolet, P.A. Houyoux, P. Cardol, B. Ghysels, S. Cuine, L. Cournac, G. Peltier, C. Remacle, F. Franck, A type II NAD(P)H dehydrogenase mediates light-independent plastoquinone reduction in the chloroplast of Chlamydomonas, Proceedings of the National Academy of Sciences of the United States of America 105(51) (2008) 20546-51.
[13] W.J. Nawrocki, N.J. Tourasse, A. Taly, F. Rappaport, F.A. Wollman, The plastid terminal oxidase: its elusive function points to multiple contributions to plastid physiology, Annual review of plant biology 66 (2015) 49-74.
[14] P. Mitchell, The protonmotive Q cycle: a general formulation, FEBS letters 59(2) (1975) 137-9.
[15] J. Alric, J. Lavergne, F. Rappaport, Redox and ATP control of photosynthetic cyclic electron flow in Chlamydomonas reinhardtii (I) aerobic conditions, Biochimica et biophysica acta 1797(1) (2010) 44-51.
[16] D. Godaux, B. Bailleul, N. Berne, P. Cardol, Induction of Photosynthetic Carbon Fixation in Anoxia Relies on Hydrogenase Activity and Proton-Gradient

Regulation-Like1-Mediated Cyclic Electron Flow in Chlamydomonas reinhardtii, Plant physiology 168(2) (2015) 648-658.
[17] K. Tagawa, H.Y. Tsujimoto, D.I. Arnon, Separation by Monochromatic Light of Photosynthetic Phosphorylation from Oxygen Evolution, Proceedings of the National Academy of Sciences of the United States of America 50 (1963) 544-9.
[18] L. Houille-Vernes, F. Rappaport, F.A. Wollman, J. Alric, X. Johnson, Plastid terminal oxidase 2 (PTOX2) is the major oxidase involved in chlororespiration in Chlamydomonas, Proceedings of the National Academy of Sciences of the United States of America 108(51) (2011) 20820-5.
[19] D. Tolleter, B. Ghysels, J. Alric, D. Petroutsos, I. Tolstygina, D. Krawietz, T. Happe, P. Auroy, J.M. Adriano, A. Beyly, S. Cuine, J. Plet, I.M. Reiter, B. Genty, L. Cournac, M. Hippler, G. Peltier, Control of hydrogen photoproduction by the proton gradient generated by cyclic electron flow in Chlamydomonas reinhardtii, The Plant cell 23(7) (2011) 2619-30.
[20] C.A. Sacksteder, D.M. Kramer, Dark-interval relaxation kinetics (DIRK) of absorbance changes as a quantitative probe of steady-state electron transfer, Photosynthesis research 66(1-2) (2000) 145-58.
[21] P. Joliot, A. Joliot, Cyclic electron transfer in plant leaf, Proceedings of the National Academy of Sciences of the United States of America 99(15) (2002) 10209-14.
[22] B. Bailleul, P. Cardol, C. Breyton, G. Finazzi, Electrochromism: a useful probe to study algal photosynthesis, Photosynthesis research 106(1-2) (2010) 179-89.
[23] K. Brettel, Electron transfer and arrangement of the redox cofactors in photosystem I, Biochimica et Biophysica Acta (BBA) - Bioenergetics 1318(3) (1997) 322-373.
[24] P. Joliot, D. Beal, A. Joliot, Cyclic electron flow under saturating excitation of dark-adapted Arabidopsis leaves, Biochimica et biophysica acta 1656(2-3) (2004) 166-76.
[25] H. Takahashi, S. Clowez, F.A. Wollman, O. Vallon, F. Rappaport, Cyclic electron flow is redox-controlled but independent of state transition, Nature communications 4 (2013) 1954.
[26] W.J. Nawrocki, S. Santabarbara, L. Mosebach, F.A. Wollman, F. Rappaport, State transitions redistribute rather than dissipate energy between the two photosystems in Chlamydomonas, Nature plants 2 (2016) 16031.
[27] S. Clowez, D. Godaux, P. Cardol, F.A. Wollman, F. Rappaport, The involvement of hydrogen-producing and ATP-dependent NADPH-consuming pathways in setting the redox poise in the chloroplast of Chlamydomonas reinhardtii in anoxia, The Journal of biological chemistry 290(13) (2015) 8666-76.
[28] G. Finazzi, F. Rappaport, A. Furia, M. Fleischmann, J.D. Rochaix, F. Zito, G. Forti, Involvement of state transitions in the switch between linear and cyclic electron flow in Chlamydomonas reinhardtii, EMBO reports 3(3) (2002) 280-285.
[29] J. Alric, Redox and ATP control of photosynthetic cyclic electron flow in Chlamydomonas reinhardtii: (II) involvement of the PGR5-PGRL1 pathway under anaerobic conditions, Biochimica et biophysica acta 1837(6) (2014) 825-34.
[30] B. Drop, M. Webber-Birungi, F. Fusetti, R. Kouril, K.E. Redding, E.J. Boekema, R. Croce, Photosystem I of Chlamydomonas reinhardtii contains nine light-harvesting complexes (Lhca) located on one side of the core, The Journal of biological chemistry 286(52) (2011) 44878-87.

[31] B. Drop, M. Webber-Birungi, S.K. Yadav, A. Filipowicz-Szymanska, F. Fusetti, E.J. Boekema, R. Croce, Light-harvesting complex II (LHCII) and its supramolecular organization in Chlamydomonas reinhardtii, Biochimica et biophysica acta 1837(1) (2014) 63-72.
[32] P. Ilik, A. Pavlovic, R. Kouril, A. Alboresi, T. Morosinotto, Y. Allahverdiyeva, E.M. Aro, H. Yamamoto, T. Shikanai, Alternative electron transport mediated by flavodiiron proteins is operational in organisms from cyanobacteria up to gymnosperms, The New phytologist 214(3) (2017) 967-972.
[33] F. Chaux, A. Burlacot, M. Mekhalfi, P. Auroy, S. Blangy, P. Richaud, G. Peltier, Flavodiiron proteins promote fast and transient O2 photoreduction in Chlamydomonas, Plant physiology (2017).
[34] C. Gerotto, A. Alboresi, A. Meneghesso, M. Jokel, M. Suorsa, E.M. Aro, T. Morosinotto, Flavodiiron proteins act as safety valve for electrons in Physcomitrella patens, Proceedings of the National Academy of Sciences of the United States of America 113(43) (2016) 12322-12327.
[35] G. Forti, G. Caldiroli, State transitions in Chlamydomonas reinhardtii. The role of the Mehler reaction in state 2-to-state 1 transition, Plant physiology 137(2) (2005) 492-9.
[36] B. Nandha, G. Finazzi, P. Joliot, S. Hald, G.N. Johnson, The role of PGR5 in the redox poising of photosynthetic electron transport, Biochimica et biophysica acta 1767(10) (2007) 1252-9.
[37] W. Yamori, T. Shikanai, Physiological Functions of Cyclic Electron Transport Around Photosystem I in Sustaining Photosynthesis and Plant Growth, Annual review of plant biology 67(1) (2016) 81-106.
[38] Y. Munekage, M. Hojo, J. Meurer, T. Endo, M. Tasaka, T. Shikanai, PGR5 Is Involved in Cyclic Electron Flow around Photosystem I and Is Essential for Photoprotection in Arabidopsis, Cell 110(3) (2002) 361-371.
[39] Y. Munekage, M. Hashimoto, C. Miyake, K.-I. Tomizawa, T. Endo, M. Tasaka, T. Shikanai, Cyclic electron flow around photosystem I is essential for photosynthesis, Nature 429 (2004) 579.
[40] X. Johnson, J. Steinbeck, R.M. Dent, H. Takahashi, P. Richaud, S. Ozawa, L. Houille-Vernes, D. Petroutsos, F. Rappaport, A.R. Grossman, K.K. Niyogi, M. Hippler, J. Alric, Proton gradient regulation 5-mediated cyclic electron flow under ATP- or redox-limited conditions: a study of DeltaATpase pgr5 and DeltarbcL pgr5 mutants in the green alga Chlamydomonas reinhardtii, Plant physiology 165(1) (2014) 438-52.
[41] W. Nawrocki, B. Bailleul, D. Picot, P. Cardol, F. Rappaport, F.-A. Wollman, P. Joliot, The mechanism of cyclic electron flow, Biochimica et Biophysica Acta (BBA)-Bioenergetics (2019).
[42] M. Iwai, K. Takizawa, R. Tokutsu, A. Okamuro, Y. Takahashi, J. Minagawa, Isolation of the elusive supercomplex that drives cyclic electron flow in photosynthesis, Nature 464(7292) (2010) 1210-3.
[43] M. Terashima, D. Petroutsos, M. Hudig, I. Tolstygina, K. Trompelt, P. Gabelein, C. Fufezan, J. Kudla, S. Weinl, G. Finazzi, M. Hippler, Calcium-dependent regulation of cyclic photosynthetic electron transfer by a CAS, ANR1, and PGRL1 complex, Proceedings of the National Academy of Sciences of the United States of America 109(43) (2012) 17717-22.
[44] J. Alric, The plastoquinone pool, poised for cyclic electron flow?, Frontiers in plant science 6 (2015) 540.

Supplementary materials:

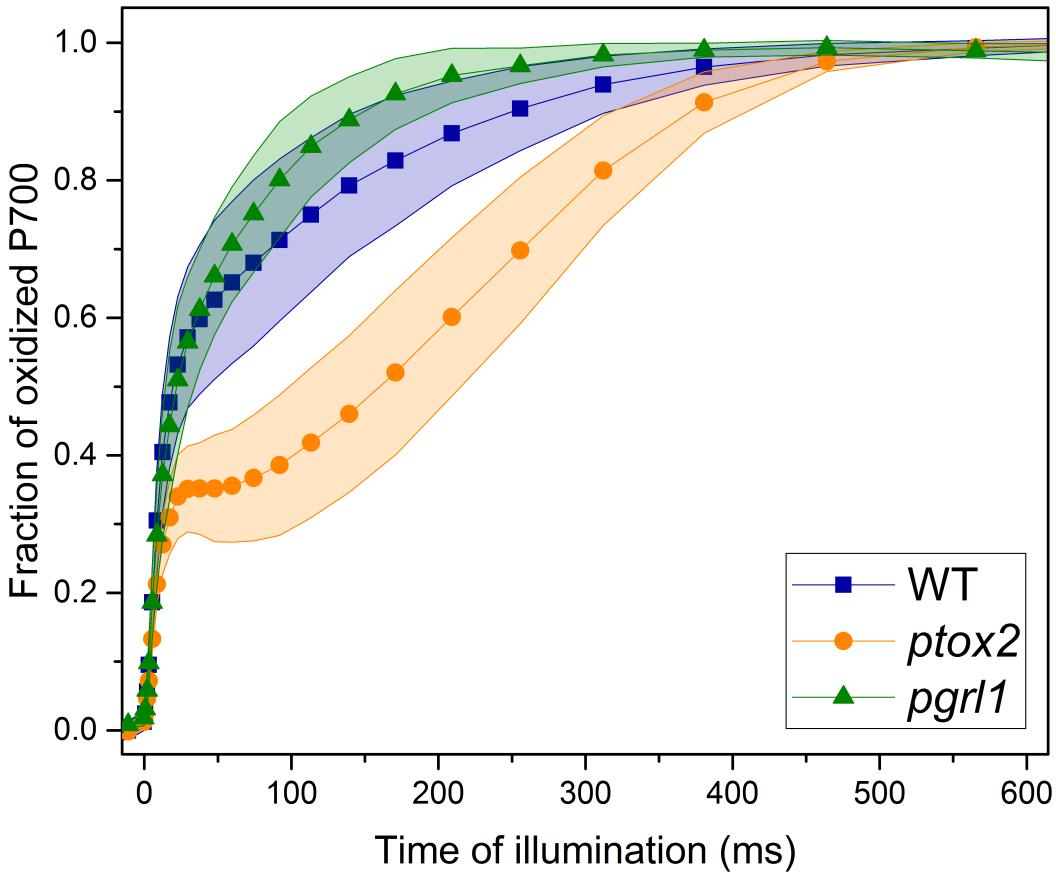

Fig. S1. Biological variability in the P_{700} oxidation kinetics in dark-adapted samples. Shaded areas correspond to the standard deviation from the mean (closed symbols) of 3 independent measurements.

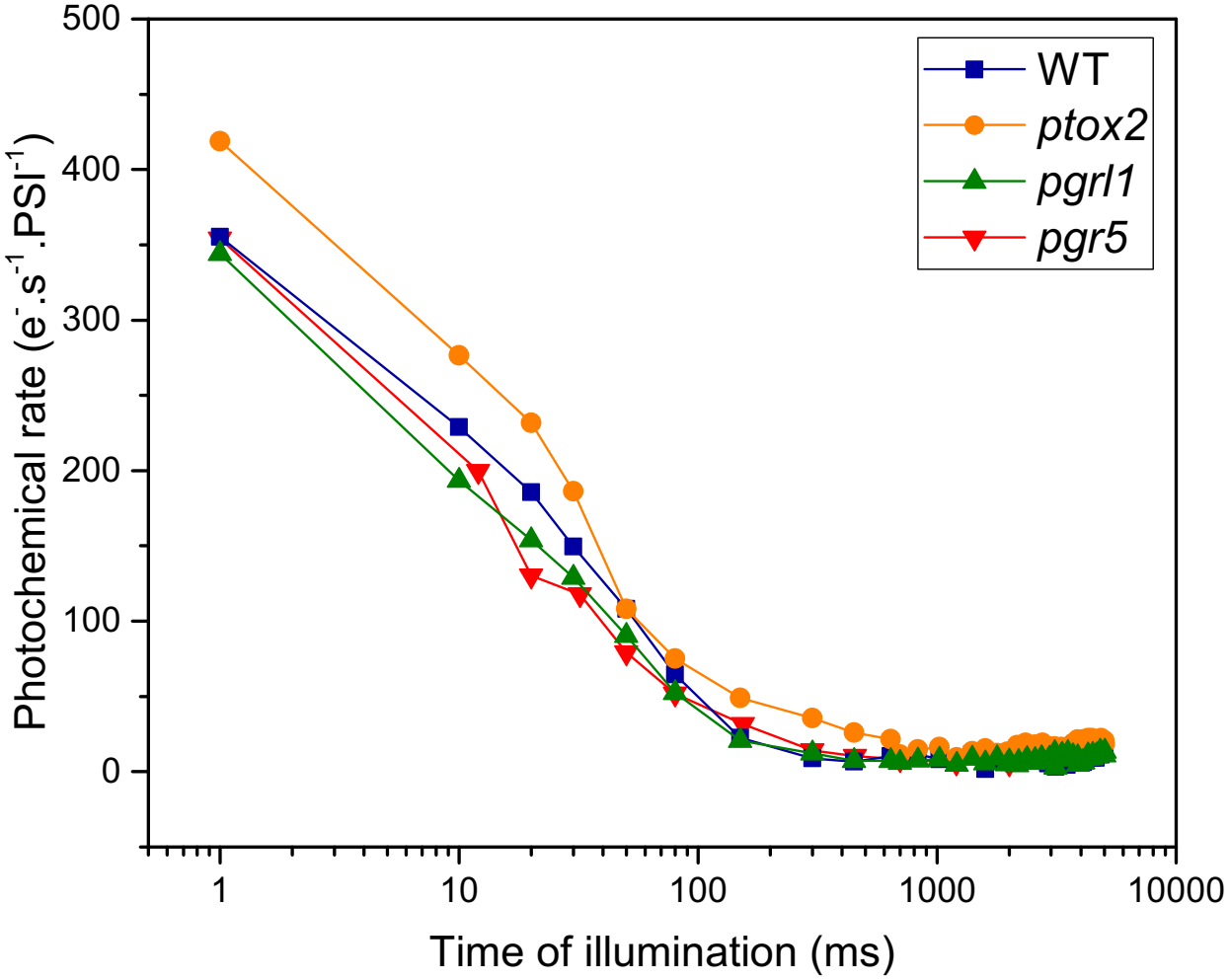

Fig. S2. *pgr5* mutant upon illumination does not significantly differ from *pgrl1*.

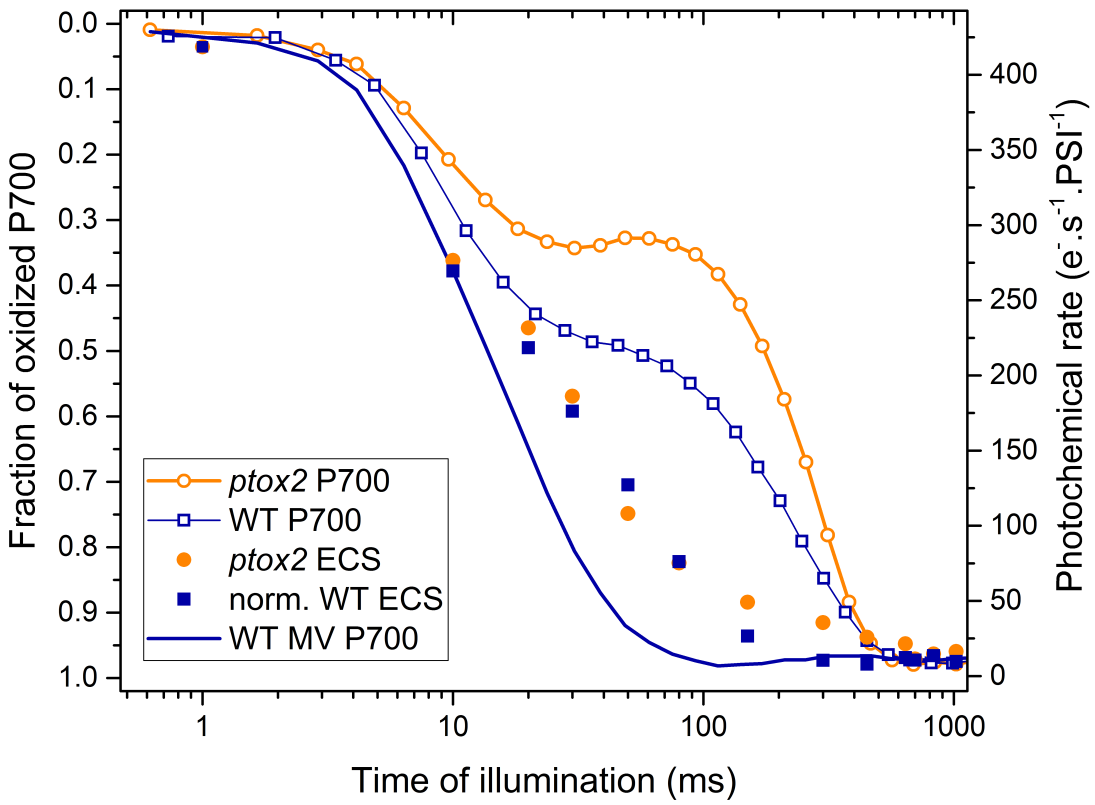

Fig. S3. Initial PSI acceptor-side limitation smoothly cedes place to CEF upon dark-to-light transition. Presented are the P_{700} oxidation traces from the Fig. 1 combined with the ECS measurements shown in Fig. 2.

Figs S4. Fluorescence induction curves in a range of oxygen concentrations. A: first and B: second phase are shown. The numbers correspond to the oxygen concentration (µM O_2) measured immediately prior to the induction curve. We note here that in order to achieve a good temporal resolution, we used lower actinic light intensity for this experiment as compared to the previous figures (~150 $e^-.s^{-1}.PSI^{-1}$). Furthermore, apart from these fluorescence measurements below, DCMU had been consistently used, the result being that the oxygen-sensitive oxidation is delayed with regards to the CEF decrease presented in the Fig. 2, the latter occurring about 100 ms after the beginning of illumination in oxic conditions. Please refer to the text for details. The curves were normalised to the maximum fluorescence level after a saturating pulse.

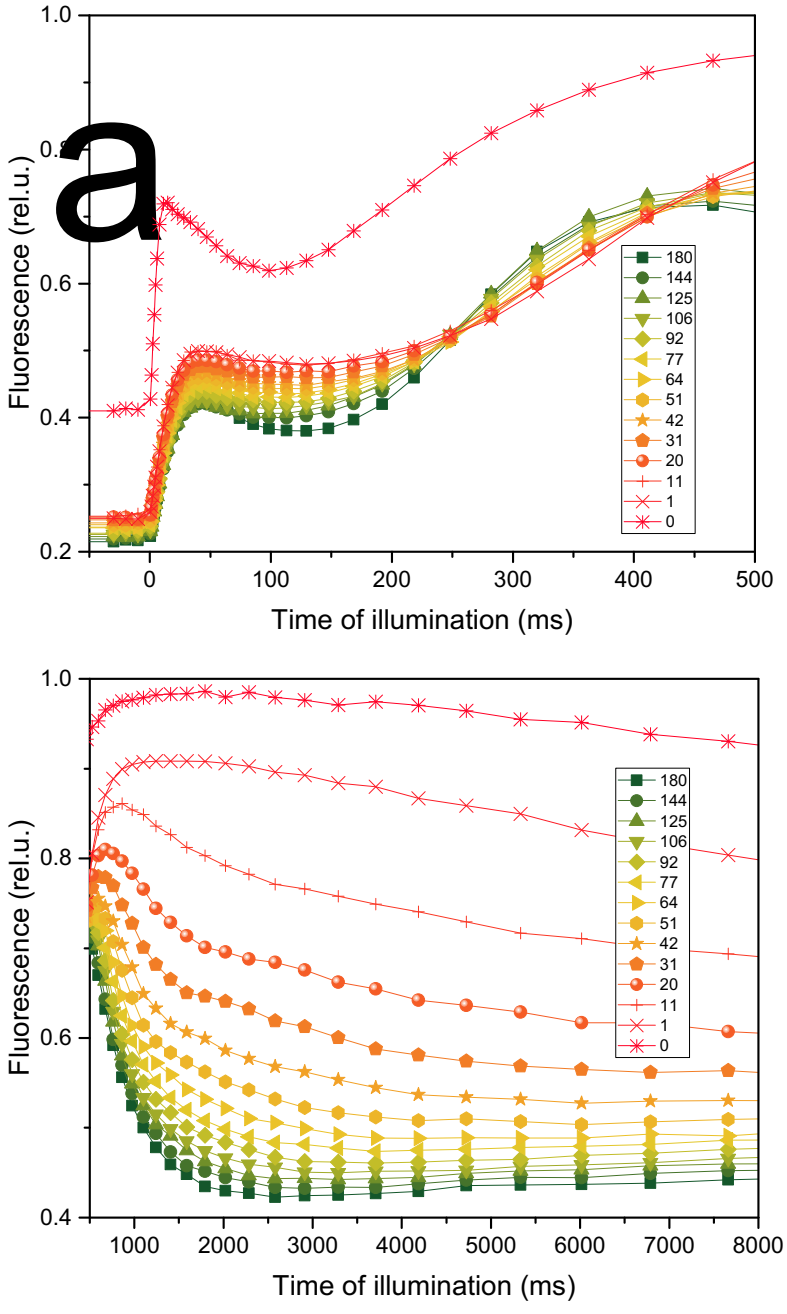

Fig. S5. Quantification of the fluorescence parameters during the transition to hypoxia of dark- and light-adapted strains. The F_M level, measured upon a saturating pulse, is normalised to 1 in final, anoxic condition (corresponding to full State II). The Φ_{PSII} ($[F_M\text{-}F_{\text{in the light}}]/F_M$) and F_V/F_M ($[F_M\text{-}F_0]/F_M$) parameters are presented as absolute values. DA, strain was dark-adapted prior to the measurement. LA, strain was in low light until directly before the measurement. A, WT. B, *ptox2*. C, *pgrl1*. D, *stt7-9*. The vertical lines in the WT graph correspond to oxygen concentrations at which the ECS measurements (Fig. 5) were done. Large differences in the F_M behaviour of the *ptox2* strain between the dark-and light-adapted situation reflect that it remains close to state II in darkness but not in the light. Note that in the *stt7-9* strain, which lacks the kinase responsible for state transitions, no changes in F_M are observed in hypoxia.

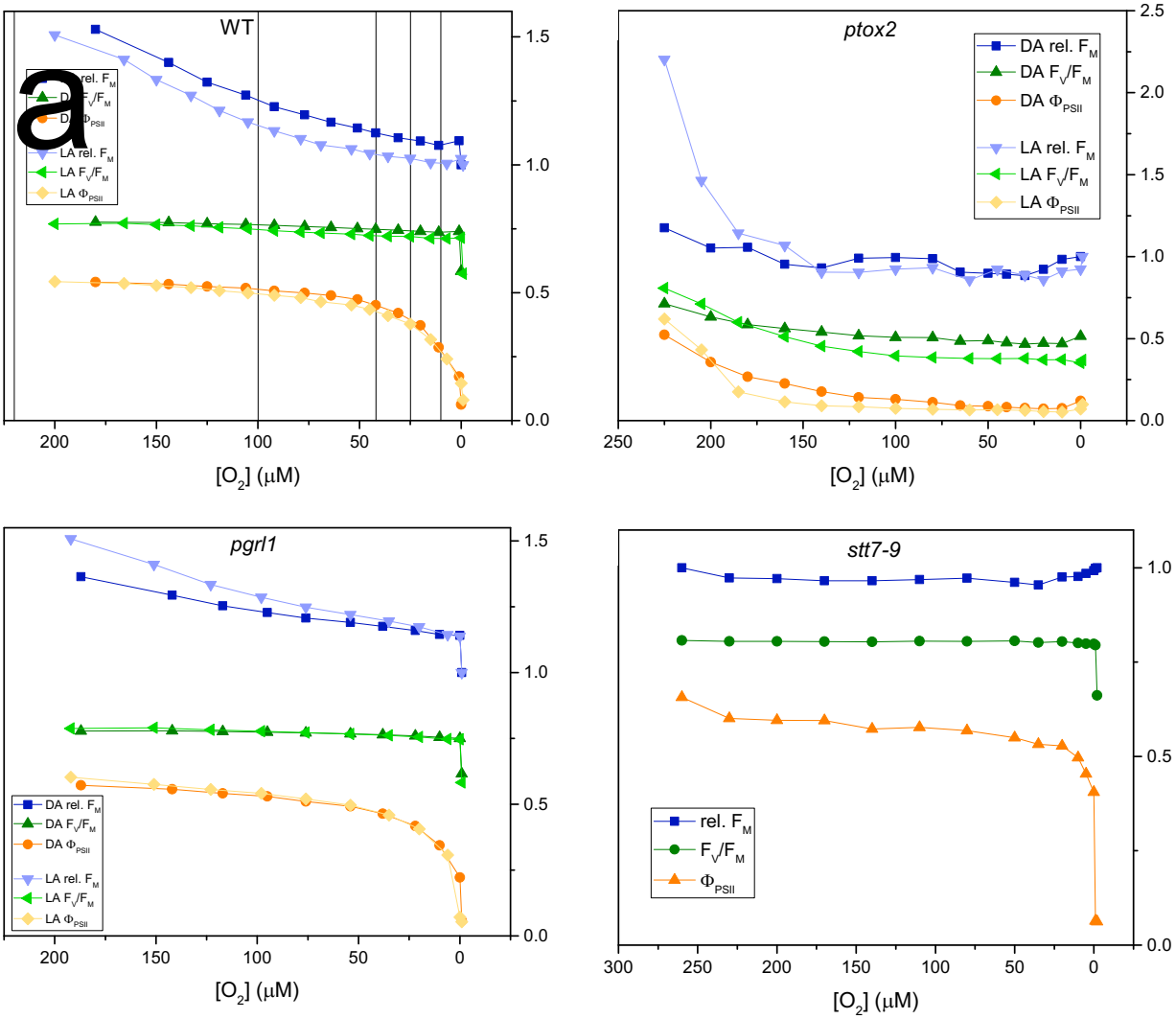

Fig. S6. Full extent of the ECS measurements in hypoxia presented in the Fig. 5. Note that logarithmic timescale had been used.